



Modelling topo-bathymetric surface using a triangulation irregular network (TIN) of Tunga Dam in Nigeria

Pius Onoja Ibrahim¹ · Harald Sternberg¹ · Hassan A. Samaila-Ija² · Donald Adgidzi³ · I. J. Nwadiolor²

Received: 15 July 2021 / Accepted: 19 April 2022 / Published online: 10 May 2022
© The Author(s) 2022

Abstract

Dams are built to store the water flowing from upstream to downstream. Sedimentation and siltation are some of the major problems affecting the storage capacity of dams. For effective management, bathymetric and topographic data are used to assess this challenge. In the Mambila Plateau of Taraba, Nigeria, the Tunga Dam is a multifunctional reservoir that serves as a small hydropower, irrigation and domestic use dam. Nonetheless, it is not operating to its full potential, leading to issues such as frequent stoppage of the turbine, low irrigation activities and a shortage of water supply for domestic use. To determine the basin's approximate present volume, a topographic and bathymetric survey was conducted using a differential global positioning system (DGPS)-Hi-Target V30 and a single beam echosounder to acquire the real-time data. The data were processed, and the digital elevation model (DEM) of the study area was modelled using a triangulation irregular network algorithm (TIN). The deepest point of the dam was found to be 21.25 m, and the volumetric capacity was assessed based on the elevations. The tessellation data format adequately represents the reservoir DEM for future purposes to better enhance the reservoir capacity. Hence, the research suggested that dredging should be carried out to boost the basin's capacity. Likewise, an embankment can be constructed around the dam to enhance the basin's storage capacity. The dredged material can be used to achieve the barrier's building, which will reduce the overall cost.

Keywords Interpolation · TIN · DEM · Bathymetry · Volume · Sounding

Introduction

Dams are constructed for collecting water to aid human activities (Keigo et al. 2006; Ferrari and Collins 2006; Ajith 2016; David 2017). Owing to the risk of sedimentation and siltation, continuous monitoring of reservoir storage capacity is necessary (EPA 1976; Carvalho et al. 2000). A more significant percentage of the sediment is trapped at the dam axis by erecting an embankment (Samaila-Ija et al. 2014; Estigoni et al. 2014; Thomas et al. 2002). Bathymetry and topography surveys are preferable approaches to determine

the bulk of sediment deposits in dams (Carvalho 1999; Chung et al. 2009; Estigoni et al. 2014; Girish et al. 2014; Ibrahim and Sternberg, 2021). Understanding dam bathymetry is critical for reservoir and environmental monitoring (Conner and Tonia 2014), with a coincident delineation of the shoreline at the instant of the survey (Khattab et al. 2017; Temitope and Kehinde 2019). Moreover, continuous and repeated observations are required to effectively impute the changes (Chia-yu et al. 2019). An adequate understanding of the morphological phenomenon around and within a water body is possible by incorporating topography and bathymetry data to produce a DEM that depicts the Earth's surface (NOAA-contributors 2007; Eakins and Grothe 2014; Amante 2018; Ludek et al. 2019). The National Oceanic and Atmospheric Administration's technical report of 2007 "Topographic and Bathymetric data considerations: Datum, Datum conversion Techniques, and data integration" focused on the methodology of providing a quality topobathy dataset to produce a DEM that meets a particular purpose. Bathymetry DEM can be used to determine the approximate volumetric capacity of the reservoir (Estigoni et al. 2014; Ajith 2016). The bulk of

✉ Pius Onoja Ibrahim
pius.onoja@futminna.edu.ng

¹ Department of Geodesy and Hydrography, Hafencity University, Hamburg, Germany

² Department of Surveying and Geoinformatics, Federal University of Technology Minna, Niger State, Nigeria

³ Department of Agricultural and Environmental Engineering, Federal University of Agriculture, Makurdi, Benue State, Nigeria

sediment material reduces the volumetric content of dams, thereby causing a shortage of supplies.

Furthermore, determining sedimentation distribution is crucial, as it affects the dam bed configuration, and the number of deposited materials is achieved via DEM (Khatab et al. 2017). DEMs also play a key role in the risk assessment of dams, such as flooding and landslides (Georgina et al. 2018). However, modelling reservoir DEMs require multiple bathymetric footprints. The instrument that can effectively carry out such a task is the multibeam echosounder and side-scan sonar. Hence, whenever a single-beam echosounder is used to acquire data, interpolation is mandatory (Samaila-Ija et al. 2014; Silverira 2014; Farrira et al. 2017). Bathymetric observations carried out using a single-beam echo sounder are deficient in footprints; therefore, the data acquired need inference to account for the sparse area to develop DEM (Lampe and Morlock 2007). In addition, the estimated output can be used to compute the reservoir storage capacity, and the rate of sediment can also be determined by cutting and filling for reference purposes (Farrira et al. 2017).

Consequently, there are different interpolation models, such as kriging, inverse distance weighting (IDW), spline and triangulation irregular networks (TIN). Each of these methods has its pros and cons. The final employment method depends on the analyst (Lark 2009).

Tunga Dam is a multipurpose dam on the Mambila Plateau, Taraba state, serving as a small hydropower source, irrigation and water supply for domestic use to neighbouring communities. The reservoir faces a frequent shortage of water in all seasons but is more pronounced in the dry season. This challenge usually results in an inadequate power supply, insufficient water supply for domestic use and poor agricultural harvest during the dry season. The purpose of this paper is to model this Tunga Dam in Nigeria using a TIN algorithm. The model will help to determine the present state of the basin and provide a possible way of increasing the volumetric capacity. Similarly, this approach will provide an approximate volume without any excessive exaggeration (Burrough and McDonnell 1998).

Study area

The study area is at Gembu, Sardauna Local Government Area of Taraba State, Nigeria. It lies in zone 33°N, within the coordinates of 741,800 mE, 762,684.76 mN; 743,061.881 mE, 761,044.723 mN; 741,827.141 mE, 759,444.698 mN and 740,184.76 mE, 761,084.76 mN (Fig. 1). The dam is seated on the Mambila Plateau in northeastern Nigeria, with a height of 2126 m above the mean sea level (MSL). The temperature in the area ranges

between 17 and 21 °C in the rainy season, perhaps one of Nigeria's coolest areas. The red arrow (Fig. 1) indicates the flow direction of the major river that supplies water to the dam. Similarly, the green arrow indicates the dam axis and the location of the road to the powerhouse. The purple line (A to B) indicates the longitudinal profile line of a sounding strip to measure the depth value at the centre of the dam.

The small hydroelectric power plant is located downstream of the reservoir with a generating capacity of approximately 400 kW. It was designed and installed by the UNIDO Regional Centre for Small Hydro Power (RC-SHP) Abuja, Nigeria. Other neighbouring communities also benefit from the generated power. These laudable and robust functionalities of the dam have necessitated continuous monitoring for adequate management. The purple line (A to B) is the longitudinal profile line, representing the centreline of the reservoir.

Materials and method

The data used in this research are topography and bathymetry data of the Tunga Dam acquired using the differential global positioning system (DGPS-) Hi-Target V30 and a single-beam echo sounder. The TIN algorithm is used to model the lake floor digital elevation model.

Topographic and bathymetry survey data

The terrain configuration of the dam was defined within the circumference of 200 m from the shoreline. Traverses of spot heights were observed at 50-m grid intervals within the offset of 200 m from the imaginary line. The topography data were measured using a DGPS Hi-Target V30 and its accessories. The observation was tied to an existing survey datum with known horizontal and vertical spatial attributes. The instrument was set up in static and real-time kinematic (RTK) mode. Thus, all the settings were configured, such as datum parameters, the source datum “WGS84/UTM zone 32 N”, the target datum “Minna/UTM zone 32 N”, which is based on Clarke 1880 ellipsoidal parameters, and the height of the instrument. It is worth noting that all the surveys are based on the Minna datum, which is the geodetic datum of Nigeria. Additionally, to minimize the errors, enough satellites (from 8 to 24) were observed with a suitable satellite geometry dilution of precision ($GDOP \leq 3$). The interreceiver path was placed at a relative distance, and both the code and the carrier phase data were ideal for observation (de Jong et al. 2003). Similarly, the highest vertical height observed during the topographic survey was 1618.635 m above mean sea level (a.m.s.l).

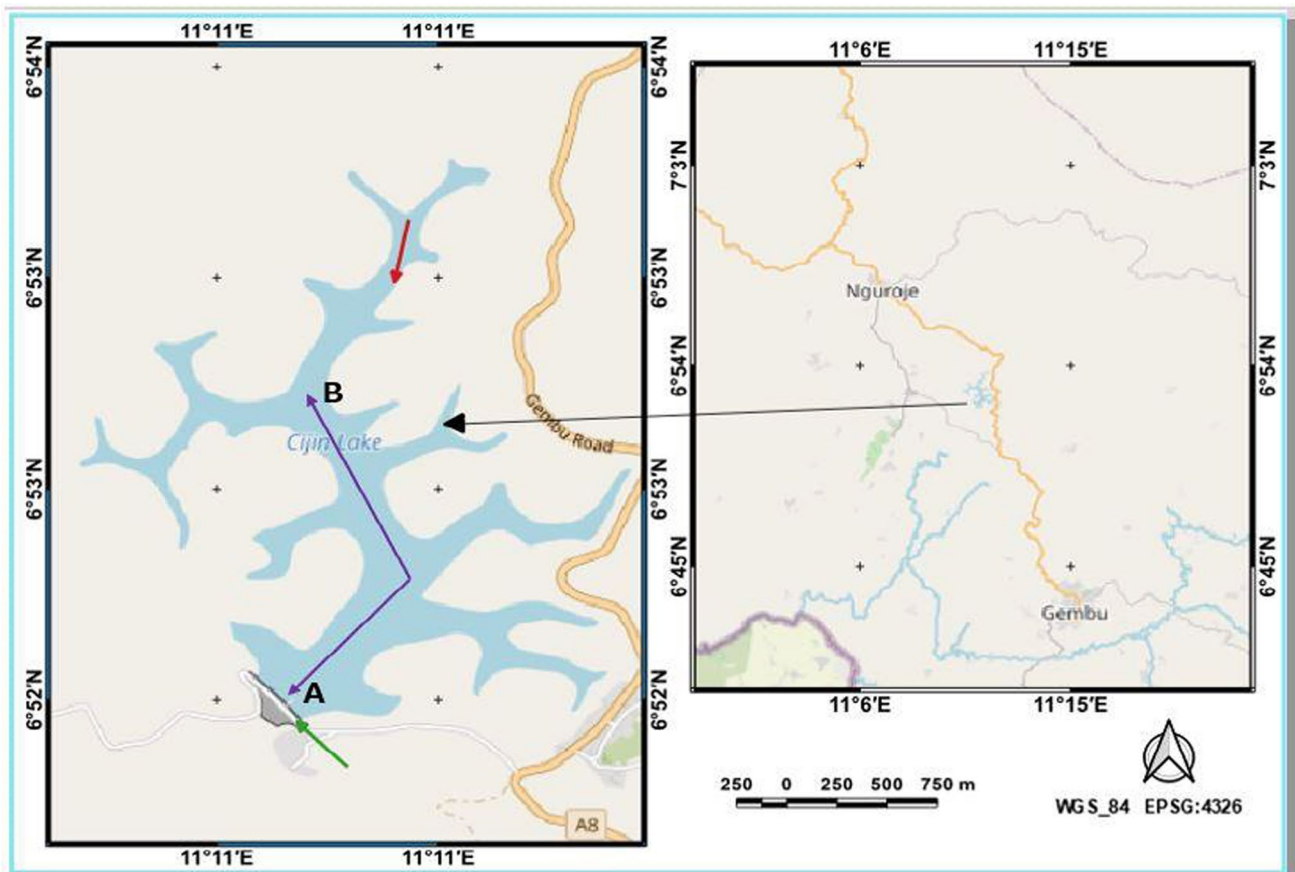


Fig. 1 Study area location (source: QGIS Google Earth Engine and Research Lab, October 2020)

Sounding operations

The process of depth determination is known as sounding. The data obtained from sounding are used to prepare a nautical chart. The act of sounding is referred to as the bathymetry survey, a survey that is synonymous with the topography survey. However, acoustic depth measurement uses the time elapsed between the propagation of an acoustic pulse from the source (transducer) to the target (seafloor) and its returns to the origin (IHO Pub. S-32; Urick 1983; de Jong et al. 2003; Xavier 2010). The travel time depends on the sound velocity. The primary constituents that affect the sound speed are salinity, temperature and pressure. The velocity changes with the variation in any of the constituents but as a function of depth (Urick 1983; Xavier 2010). Figure 2 is a graph of sound velocity against temperature; it illustrates the sound speed at different temperatures.

The maximum velocity is obtained at 70 °C, and it drops as the temperature increases (refer to Fig. 2). If the sound velocity (v) and time (t) in which it takes to propagate to and from the water column are known, then the depth (D) can be computed using the following equation (Urick 1983):

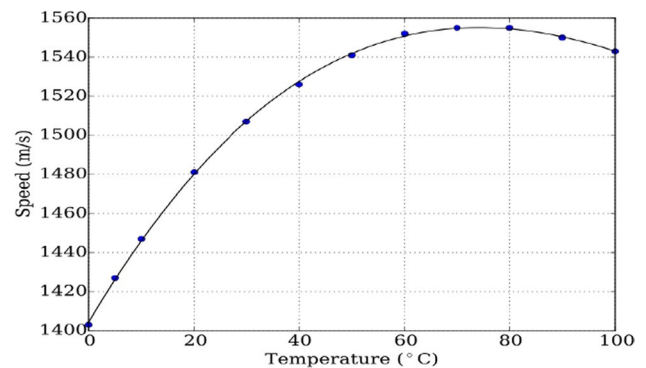


Fig. 2 Sound velocity against temperature (source: Wong and Zhu, 1995)

$$D = 1/2(v \times t) \tag{1}$$

It can be inferred from Eq. (1) that depth (D) is directly proportional to half the product of average velocity (v) and time (t). When the velocity and time are constant and equal, the depth observed will be similar, resulting in a flat surface. If the average velocity of sound propagation in the water

column is known, along with the distance between the transducer and the reference water surface, the corrected depth (d) can be computed by the pulse's measured travel time. The corrected depth is computed using Eq. (2).

$$d = 1/2(v.t) + k + dr \quad (2)$$

where d indicates the corrected depth from the reference water surface; v is the average velocity of sound in the water column; t denotes the measured elapsed time from the transducer to the bottom and back to the transducer; k is the system index constant; and dr indicates the distance from the reference water surface to the transducer (draft) (SBADMT 2002).

This research's bathymetric data are obtained using EchoMap 50 s (single beam sounder). This instrument is designed to give x , y and d i.e. easting, northing and depth data, respectively, and the datum must be specified during the data acquisition (in this case, the Minna datum is used). A constant value of sound velocity in freshwater is adopted for the operation. The sound velocity in freshwater is observed to be 1498 m/s at 25 °C with a density of 0.998 g/cm³ (Urlick 1983) and is supported by Fig. 2. However, the uncertainty in measurements affects the accuracy of the DEM, if not corrected.

To further improve the accuracy of the depth measurement, vertical and horizontal uncertainty is taken into account. A detailed review of uncertainty can be found in IHO C-13; Hare et al. (2011). To minimize and control the possible errors during data acquisition, the transducer is kept vertically and horizontally stable to avoid tilt. The transducer's constant depth is 0.326 m below the water surface; a bar check is conducted to confirm that the instrument is in a good state and fit for the task. Additionally, the value of the transducer depth below the water level is later added to each observed depth to obtain the actual depth. Reduced depth is the final depth after considering all the anomalies and correcting them during and after the

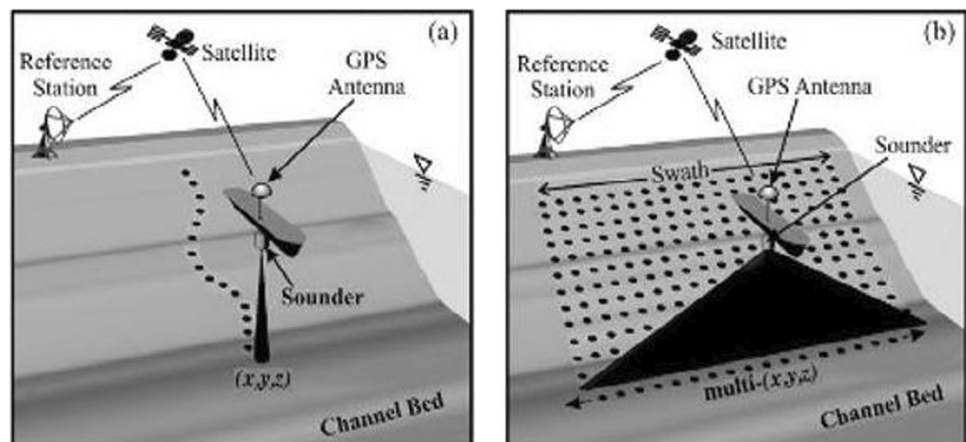
observations (de-Jong et al. 2003). Consequently, measured depths should be referenced to a chart or survey datum by applying tidal or water level height (Ingham 1984; de-Jong et al. 2003; Samaila-Ija et al. 2014). It is worth noting that the area of the study is less tidal. The vertical sounding datum to which all the depths are referred is 1581.593 m a.m.s.l.

Interpolation

Interpolation is the act of using a discrete set of known data points to estimate an unsampled area using mathematical and statistical functions (geostatistical techniques) but within the conferment of the original dataset (Landim 2000; Childs 2004; Marcelo et al. 2015; Farrira et al. 2017). One of the deterministic techniques used in this research is triangulation irregular networks (TINs). Interpolation is mandatory to account for the areas that are neglected intentionally or unintentionally during data acquisition. Figure 3 illustrates the footprint of a single-beam and multibeam echosounder.

The data obtained using Fig. 3(b) technique efficiently defines the seafloor configuration. On the contrary, information derived from Fig. 3(a) will be interpolated to effectively represent the waterbed digital elevation model. Consequently, the interpolation method to be adopted depends on the analyst as well as the purpose of estimation. Hence, the triangulation irregular network (TIN) was adopted. The TIN method uses the dataset to form a series of joint triangles that are contiguous (Burrough, 1987). Each of these triangles is a space called the plane. This plane represents the surface morphology of the object under investigation (Lee 1991; Burrough and McDonnell 1998; Floriani and Magillo 2009; El-Hattab 2014). The mathematical model can be found in Floriani and Magillo (2009).

Fig. 3 Echo sounders footprint (a) single-beam, (b) multibeam (source: Marian et al. 2012)



Area and volume computation

The entire area traversed during the survey, and the section covered by the dam is computed using the spatial cross coordinate method. There are several other methods of determining areas, such as the midpoint ordinate rule, trapezoidal rule, graphical rule, average ordinate rule and Simpson’s rule. However, the method adopted here is the spatial cross coordinate method, which is given as: Eq. 3

$$Area (m^2) = \frac{1}{2}(N_1E_2 - E_1N_2 + N_2E_3 - E_2N_3 \dots + N_nE_1 - E_nN_1) \tag{3}$$

where *N* and *E* represent the northings and eastings of the network in consideration, respectively. The subscript is the point number (Samaila-Ija et al. 2014). Furthermore, Simpson’s rule is used to compute the volume of the dam as surveyed. This volume determination method is based on cubic interpolation instead of quadratic interpolation, as demonstrated in the following equation:

$$Volume (m^3) = \frac{3h}{8} \{f(X_0) + 3f(X_1) + 3f(X_2) + f(X_3) + f(X_3) + 3f(X_4) + 3f(X_5) + f(X_6) + \dots + f(X_{n-3}) + 3f(X_{n-2}) + 3f(X_{n-1}) + f(X_n)\} \tag{4}$$

Eventually, Eq. (4) can be rounded off as: Eq. 5

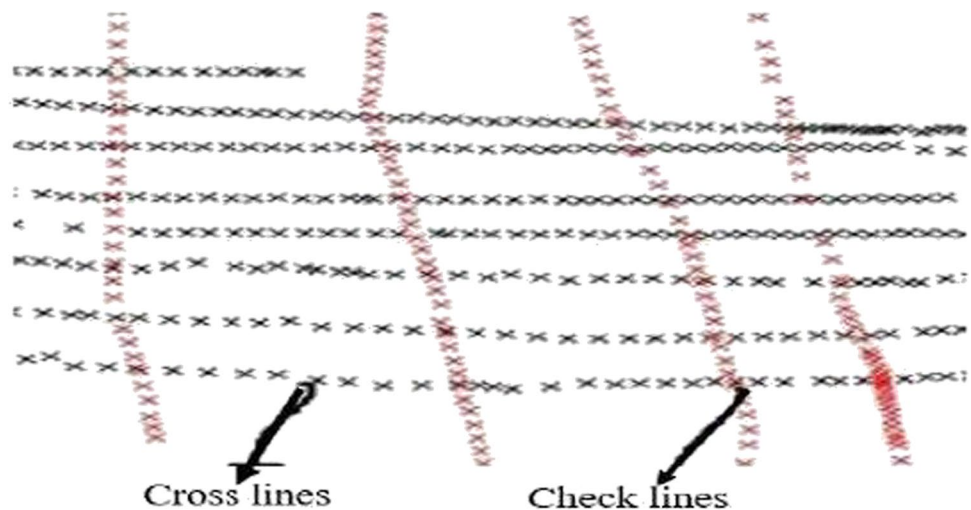
$$Volume (m^3) = \frac{3h}{8} \{f(X_0) + 3\sum_{i=1,4,7}^{n-2} f(X_i) + 3\sum_{i=2,5,8}^{n-1} f(X_i) + 2\sum_{i=3,6,9}^{n-3} f(X_i) + f(X_n)\} \tag{5}$$

where *n* indicates the number of segments; *h* represents the vertical distance or elevation (in this case, the reduced depth); and *X* is the area. Similarly, the reservoir capacity curve is determined using Eq. (6).

$$V_y = k + my + ny^2 \tag{6}$$

where *V_y* is the reservoir capacity at depth *y*; *y* is the observed depth from the water surface to the dam bed; and *k*, *m* and *n* denote the coefficients (Kaveh et al., 2013).

Fig. 4 Sounding strips (cross lines) and profile lines (check lines)



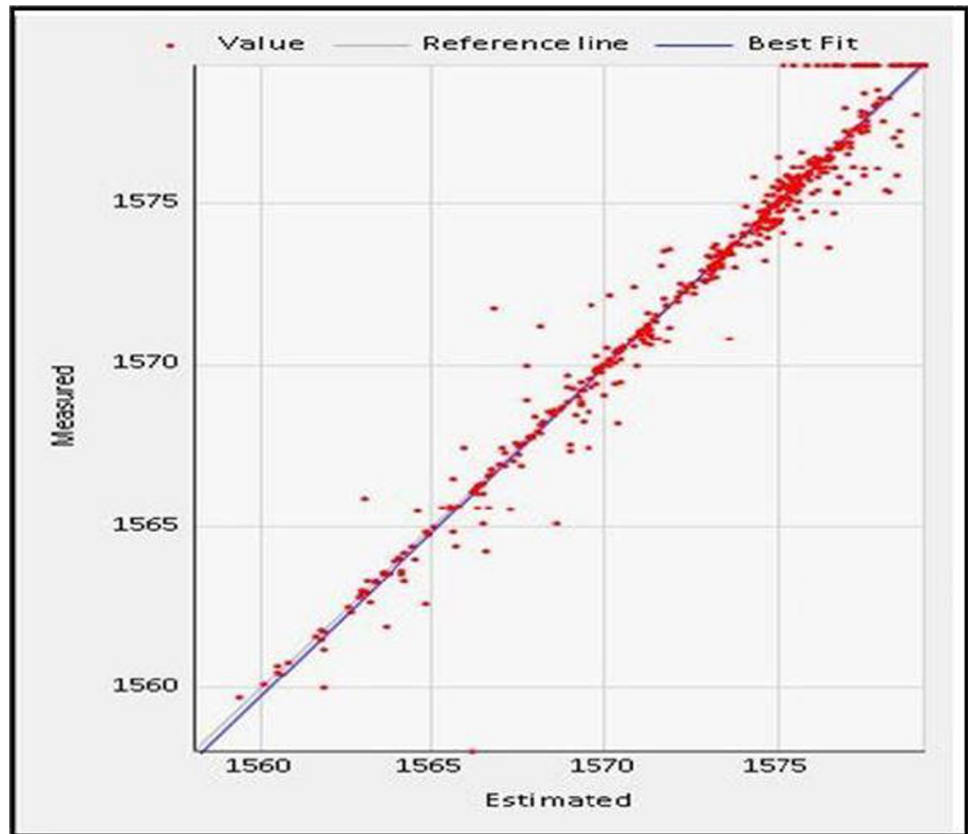
TIN DTM measure of evaluation

The TIN methodology is a triangular-based DEM system (Olender 1980). The resulting mesh is a suitable representation of the terrain configuration with adequate spread point data (Amante and Eakins 2016). However, to ascertain the accuracy of the lake floor DEM, some validation procedures need to be applied to the data. In addition, positional and vertical errors need to be adequately considered during data acquisition and processing to eliminate/reduce the effects of systematic bias, blunders and random errors on the final DEM. In particular, independent data that are not a part of the estimation data must be used to test the positional accuracy. Preferably, these data should be acquired using a different instrument (Wechsler 2007; EL-Hattab 2014). Thus, the difference between the independent and estimated depths is computed, and the residual is analysed. Figure 4 illustrates cross lines and check lines. Check lines are profile lines

observed perpendicular to the cross line/sounding strips to determine the positional accuracy of the data.

Consequently, the discrepancies between the main survey strips, and the check lines must be within the required survey order (CHS 2005). When the change exceeds the required specification, proper observation(s) should be conducted to determine the error source(s). As soon as the source of misclosure is identified, correction should be applied before further processing (El-Hattab 2014). Another DEM accuracy assessment used is the intentionally omitted depth/split-sample method before estimation, as highlighted in Fig. 5. These points are omitted before interpolation, and their spatial attributes

Fig. 5 Randomly selected 400 points for cross-validation



are compared after estimation. Figure 5 demonstrates the cross-validation of measured and estimated points in red and is randomly selected by the algorithm. The selected points are plotted against the original dataset to check their spread.

Consequently, there should be a strong correlation between the two datasets; otherwise, the interpolation process needs to be verified for possible errors. Furthermore, a quantitative measure of accuracy, such as the mean error (ME), mean squared error (MSQ) and root mean squared error (RMSQ), should be used to calculate the degree of bias and error size in the output. Ahmed and De Marsily (1987), Burrough and McDonnell (1998), Hu et al. (2004), Isaaks and Srivastava (1989), and Vicente-Serrano et al. (2003) gave the mathematical expressions as follows:

$$MSE = \frac{1}{n} \sum_{i=1}^n (\hat{Z}_i - Z_i)^2 \quad (7)$$

$$RMSE = \sqrt{\frac{\sum_{i=1}^n (\hat{Z}_i - Z_i)^2}{n}} \quad (8)$$

where Z_i = observed value, \hat{Z}_i = the predicted value and n = the total number of points considered in Eq. (7) and Eq. (8), respectively.

The mean error can be computed as: Eq. 9

$$ME = \frac{\sum_{i=1}^n (Z_i^{PRED} - Z_i^{OBS})}{n} \quad (9)$$

where Z_i^{PRED} and Z_i^{OBS} represent the predicted and observed depths, respectively, and n is the total number of samples. The statistical models are used to test the experiment's performance; when they tend to zero, it represents the reliability of the interpolation technique.

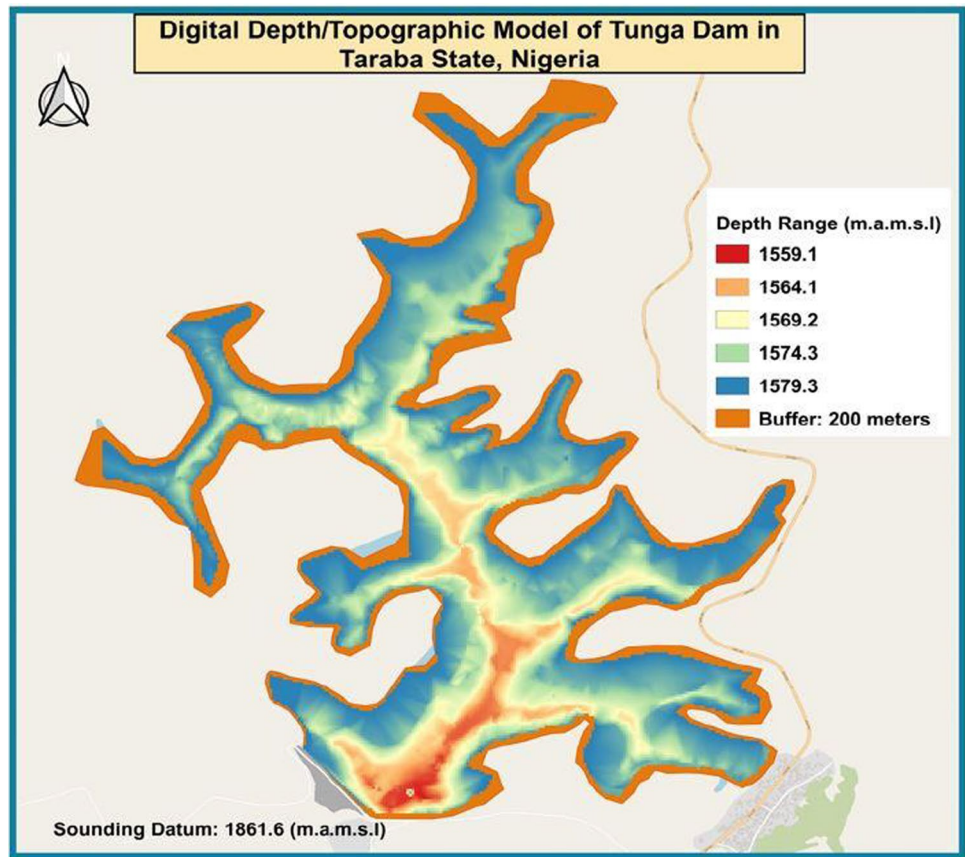
Results and analysis

The maximum depth of the dam obtained from sounding is 21.25 m. The maximum and minimum elevations, as referenced to mean sea level, are 1579.30 m and 1558.05 m, respectively. Table 1 highlights the performance results of the check lines and cross-validation used for the DEM

Table 1 Cross-validation and omitted points (unit meter)

	ME	MSE	RMSE
Cross-validation	0.102	0.126	0.354
Check lines/cross lines	0.107	0.043	0.204

Fig. 6 Composite DEM of bathymetric and topographic surfaces



accuracy assessment. The result (Table 1) describes a small divergence in the mean error (ME), mean square error (MSE) and root mean squared error (RMSE).

Similarly, the evaluation shows that both datasets’ degrees of bias agree, but with a small difference of 0.005. In contrast, the large difference in the measurement of error size (RMSE) between the cross-validation and the omitted points indicates the weight of MSE. When ME and MSE tend to zero and RMSE is smaller, the interpolation technique proves to be excellent (Li and Heap 2008). Figure 6 shows the composite digital depth model (DDM) of the study area. It shows the topography terrain in brown and the water body in colour range, and it becomes faint as it expands towards the shoreline. In addition, at the legend is the depth range referred to as m.s.l. To obtain the depth value, the reduced depth is subtracted from the vertical sounding datum value.

The highest point above the mean sea level observed on the terrain is 1618.635 m. In addition, the total surveyed area (Topo) surveyed is 3,716,941.615 m² with a perimeter of 22,829.345 m. Additionally, the area covered by the reservoir is 1,314,327.81 m² with a perimeter of 23,201.361 m. From the perimeter computed, it will be observed that the shoreline perimeter, which is a subset of the entire surveyed area, is higher than that of the total area calculated; this is due to the meandering nature of the shoreline. Additionally, this is because the perimeter is a function of a traverse path followed during the survey operation. Furthermore, the total triangles in the model are 16,753, with maximum and minimum triangle areas of 4156.06 m² and 0.08 m², respectively. Similarly, the maximum and minimum triangle lengths are 132.488 m and 0.292 m, respectively. This is listed in Table 2. The

Table 2 TIN surface characteristics

TIN	Extended
Number of triangles = 16,753	2D surface area = 1,314,327.81 m ²
Maximum triangle area = 4165.06 m ²	3D surface area = 1,337,713.37 m ²
Minimum triangle area = 0.08 m ²	Mini grade/slope = 0.00%
Minimum triangle length = 0.292 m	Maximum grade/slope = 74.45%
Maximum triangle length = 132.488 m	Mean grade/slope = 2.62%

maximum triangle length is obtained from the hazard terrain of some sections of the study area that are difficult to access during the sounding operation. This length confines the maximum area of the triangle and accounts for 0.32% of the total water body area surveyed.

The three-dimensional (3D) surface area is the space covered by the triangles in the DEM defined by nodes and edges, as illustrated in Fig. 7(a) and (b). The total 3D surface area of the DEM is 1,337,713.37 m², and it is highly correlated with the one computed from a different model, as mentioned in Table 3. The lower and higher slope inclinations

of the terrain are 0% and 74.45%, respectively. This shows the steepness of the waterbed based on the surface characteristics of the DEM. To avoid vertical exaggeration, the steepness is computed using a Z-factor of 1. If the Z-factor exceeds 1, it will increase steeply above the raw data steepness.

Consequently, the profile and cross-section data create brake lines for triangles and vertices within and around the surface, which accurately define the surface morphology (Guo et al. 2010). This assertion is supported by Figs. 7(b) and 8, respectively. Another

Fig. 7 (a) TIN surface with nodes and edges, (b) shaded TIN surface (source: research lab)

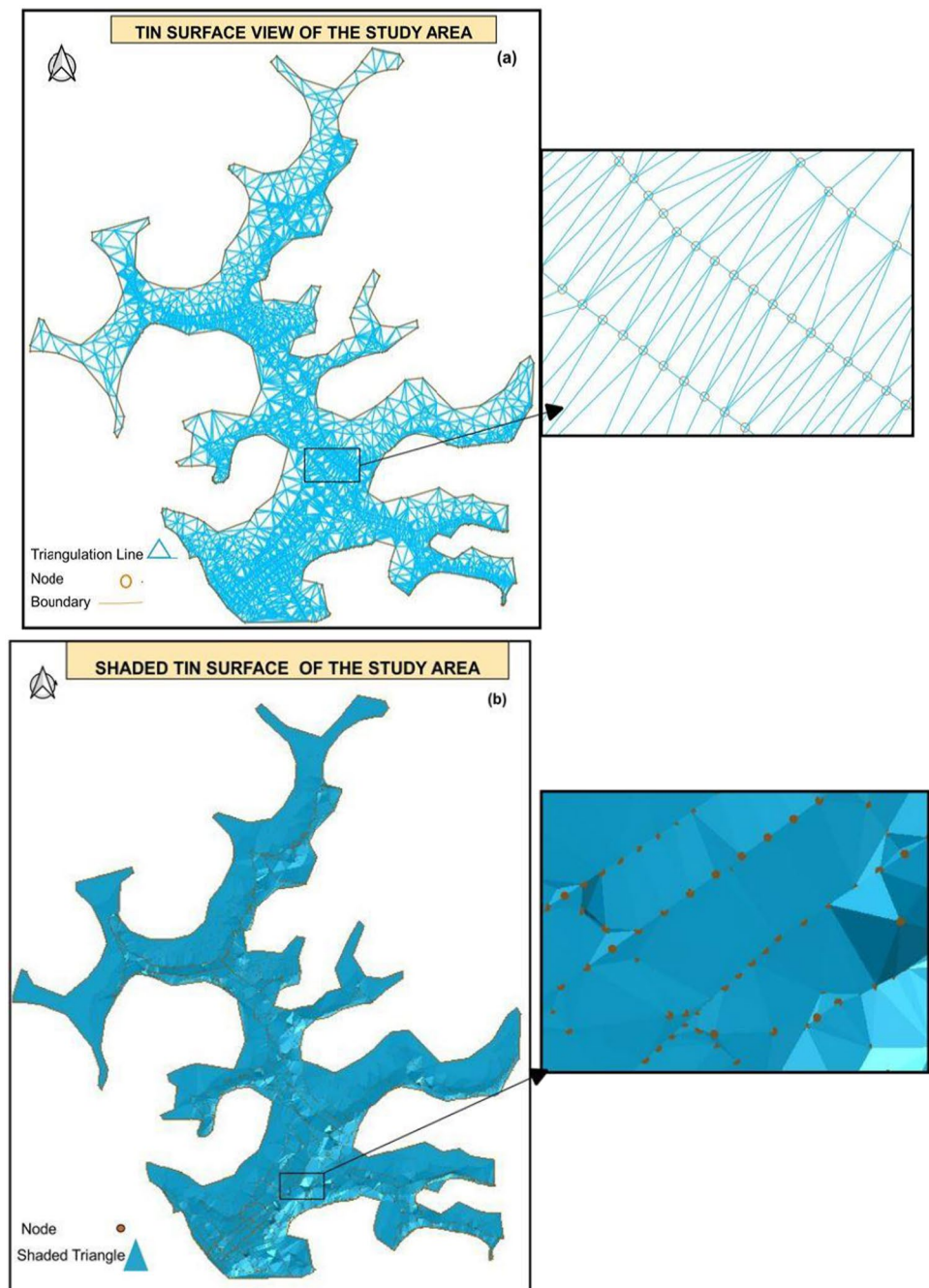


Table 3 Elevation analysis results. Sounding datum: 1581.6 m; waterlevel: 1579.3m

Minimum Elevation (m)	Maximum Elevation (m)	Colour Scheme	2D Area	3D Area	Volume
1558.05	1566.02		142940.32	144672.00	10120684.01
1566.06	1569.74		201113.01	203969.30	4010177.74
1569.76	1571.76		151852.63	154189.27	1813971.87
1571.76	1573.63		175357.43	178387.92	1373124.58
1573.63	1575.20		166479.09	169629.54	877695.20
1575.20	1576.41		117873.97	120728.67	505178.06
1576.41	1579.30		358711.35	366136.67	638796.18
		Total output	1314327.80	1337713.37	19339627.64

*Non-Hispanic Other includes Native Hawaiian/Pacific Islander, Non-Hispanic Other race only/Non-Hispanic Multiracial

factor that is used to control the output of the TIN DTM is the shoreline delineation. This is in concordance with Amante and Eakins (2016), who found that creating a data buffer around the study area minimizes edge effects in the interpolated DEM. This prevents the TIN surface from overlapping, as highlighted in Figs. 7(a) and 8. When there is an overlap with the neighbouring surfaces, it will result in a false DEM surface and incorrect triangles with vertices. Alternatively, Table 3 shows the outcome of elevation analysis.

Figure 8 represents the tessellation output of the study area, and it highlights the connecting channels. The tributary channel eroded the sediment from upstream and adjoining rivers into the reservoir. These flooded particles are further trapped at the reservoir axis. The impounded sediments reduce the storage capacity over time, thereby affecting its functionality. The volume of the raster DEM of Fig. 8 is computed to be 23,026,735.864 m³, which is in contrast with the total

volume in Table 3. An error can be introduced when transforming TIN (polygon) to the raster data format (Hengl 2007; Amante and Eakins 2016). Assessing such errors is not within the scope of this paper. However, the raster format adequately represents the TIN DEM surface when the cell size is reduced (ESRI 2010c). The total reservoir capacity mentioned in Table 3 is based on the TIN vector output in Fig. 7(a).

The reservoir capacity curve

Area capacity curves help in better understanding a reservoir's condition in terms of reservoir operation, flood routing, determination of water surface area, and content about each elevation or depth, sediment distribution and reservoir classification (Jahanshir et al. 2009). The reservoir area capacity curves based on the information in Table 1 are shown in Fig. 9. The blue and orange

Fig. 8 TIN raster DEM of the study area (source: research lab)

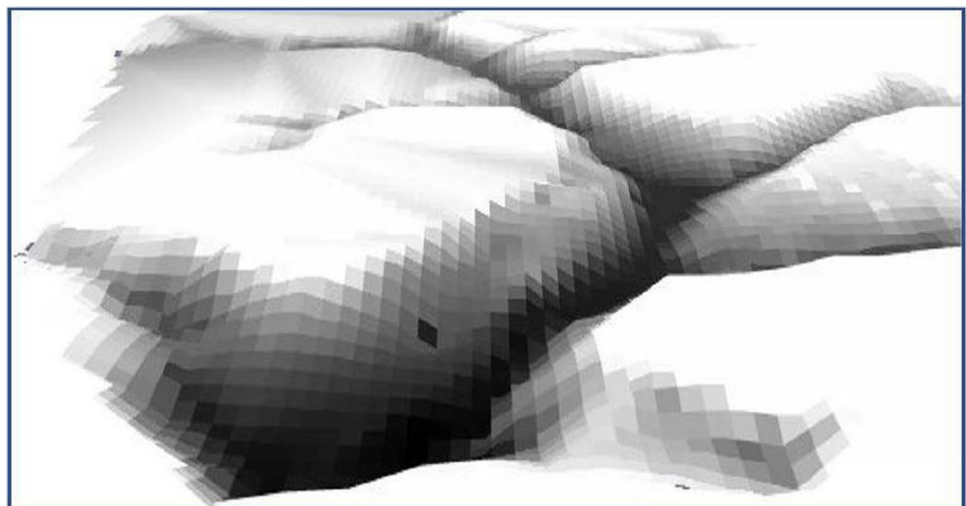
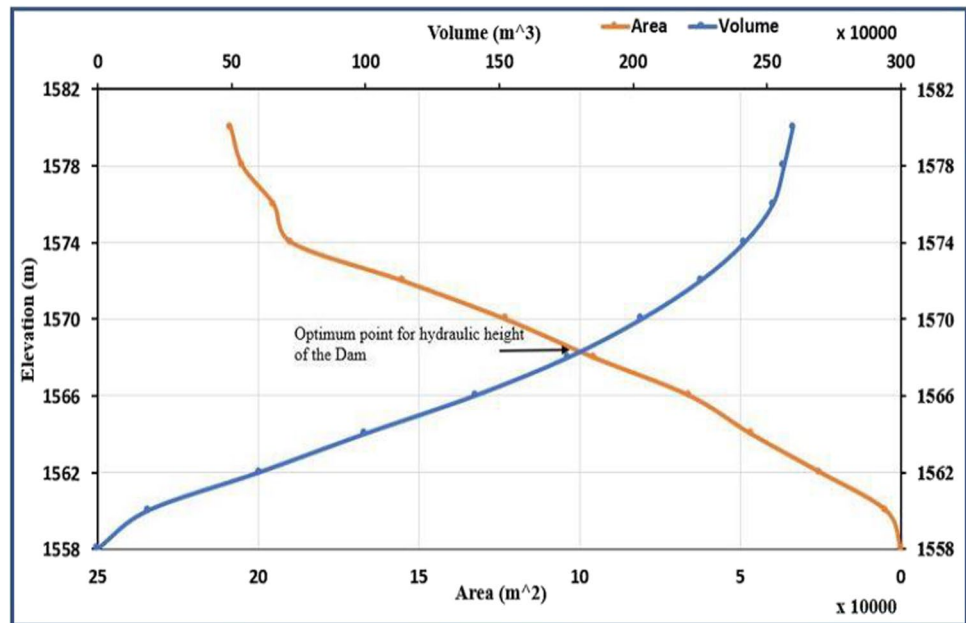


Fig. 9 Reservoir capacity curve of the dam



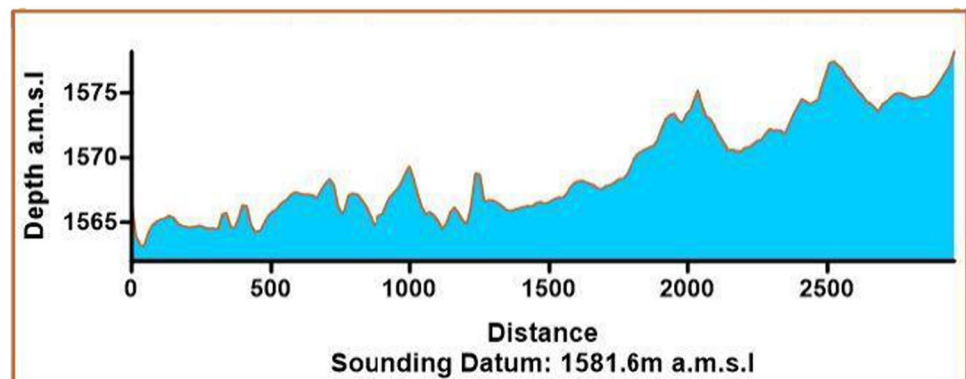
traverse lines indicate volumes and areas at the elevation classification of two-meter (2 m) interval. Additionally, the dots highlighted in Fig. 9 are the points of relationship between area and elevation and volume and elevation. It is evident that as the area increases, the volume also increases with respect to height.

In Fig. 9, the intersection between area and volume indicates the optimum point for the dam's hydraulic height. This point intersects at an elevation of 1568.500 m with a volume and area of 2,163,972.62 m³ and 120,247.12 m², respectively. This is approximately 11.19% and 9.15%, considering the entire volume and area listed in Table 3. This is evidence that the dam is not operating at its full capacity. The utmost hydraulic capacity is lost to sedimentation and siltation. Figure 9 supports this assertion with the irregular curves, mainly the area curve. Another factor that collaborates with this is the slope

factor, as mentioned in Table 2, which shows a sharp fall at the dam axis. The dam morphology also contributed to this problem, since it does not have efficient depths at the supply channels. The dam functions because of the gradual and constant flow of water from the catchment areas. Additionally, Fig. 10 represents the longitudinal sounding strip from the dam axis to the major catchment, as described in Fig. 1. This is described from upstream to downstream in Fig. 10. The sloppy nature of the dam bed explains why sediment accretion is mostly observed at large magnitudes along the reservoir axis.

Similarly, the surface configuration is an indication that the area is rocky, which might have served as a hindrance or obstacle during the construction. On average, the dam is approximately three kilometres (3 km) in length and two hundred and twenty-five meters (225 m) in width.

Fig. 10 Longitudinal sounding strip (source: Research lab)



Conclusion

The combination of bathymetry and topography data to model the DEM of a water body aids the understanding of the geomorphological phenomenon for adequate planning and monitoring (Amante and Eakins 2016). Thus, the TIN algorithm was successfully used to develop the DDM of the Tunga Dam. The DDM indicates the meandering nature of the dam, as shown in Figs. 8 and 9. The topography of the Mambila Plateau is mountainous with valleys within its surroundings. The bathymetric survey highlights the dam depth distribution and the effects of sedimentation. The depth information suggests that the reservoir requires dredging. However, there is no construction information about the dam to ascertain the decrease in depth from accretion that emanated from sedimentation and siltation, which is a function of time. The DDM of the study area revealed that the dam demands urgent maintenance. The researchers suggest that management should dredge the dam. However, this is a difficult or impossible task owing to the lake floor's potential geological variability, which is also quite expensive for the lake's overall surface. Shallow dredging can be performed, and a barrier can be constructed to enhance the basin's storage capacity. This information can be used as a future basis for the study of this research area.

Acknowledgements The authors sincerely acknowledge the United Nations Industrial Development Organization (UNIDO) team in Abuja, for her support during the field research work. The authors also appreciate the Taraba State Government for providing the enabling environment for the team. Additionally, thanks go to all other survey team members.

Author contribution Each author played a separate role during data acquisitions and processing, except for the second co-author (H. S.) who is the supervisor of the leading author. The corresponding author is a PhD student under the supervision of H. S.

Funding Open Access funding enabled and organized by Projekt DEAL.

Declarations

Data availability The datasets generated during and/or analysed during the current study are available from the corresponding author on reasonable request.

Compliance with ethical standards This article adhered to all relevant ethical standards.

Ethical approval This study does not involve any studies with human participants or animal experiments.

Informed consent Informed consent was obtained from all the individual participants or third party included in the study.

Conflict of interest The authors declare no competing interests.

Open Access This article is licensed under a Creative Commons Attribution 4.0 International License, which permits use, sharing, adaptation, distribution and reproduction in any medium or format, as long as you give appropriate credit to the original author(s) and the source, provide a link to the Creative Commons licence, and indicate if changes were made. The images or other third party material in this article are included in the article's Creative Commons licence, unless indicated otherwise in a credit line to the material. If material is not included in the article's Creative Commons licence and your intended use is not permitted by statutory regulation or exceeds the permitted use, you will need to obtain permission directly from the copyright holder. To view a copy of this licence, visit <http://creativecommons.org/licenses/by/4.0/>.

References

- Ahmed S, De Marsily G (1987) Comparison of geostatistical methods for estimating transmissivity using data on transmissivity and specific capacity. *Water Resour Res* 23(9):1717–1737. <https://doi.org/10.1029/WR023i009p01717>
- Ajith AV (2016) Bathymetric survey to study the sediment deposit in reservoir of Peechi Dam. *IOSR J Mech Civil Eng* 12(6):34–38. <https://doi.org/10.9790/1684-12644143>
- Amante CJ (2018) Estimating coastal digital elevation model uncertainty. *J Coastal Res* 34(6):1382–1397. <https://doi.org/10.2112/JCOASTRES-D-17-00211.1>
- Amante CJ, Eakins BW (2016) Accuracy of interpolated bathymetry in digital elevation models. In: Brock JC, Gesch DB, Parrish CE, Rogers JN, Wright CW (eds.): *Advances in topobathymetric mapping, models, and applications*. *J Coastal Res* 76: 123–133. Coconut Creek (Florida). <https://doi.org/10.2112/SI76-011>
- Burrough PA (1987) Principles of geographical information systems for land resources assessment. *Int J Geogr Inf Syst* 1(2):189–190. <https://doi.org/10.1080/02693798708927804>
- Burrough PA, McDonnell RA (1998) *Principles of geographical information systems*. Oxford University Press, Oxford England
- Canadian Hydrographic Service (CHS) (2005) *CHS Standards for hydrographic surveys first edn Fisheries and Oceans, Canada*. <https://www.charts.gc.ca/index-eng.html>
- Carvalho NO (1999) Reservoir sedimentation effects on hydropower generation—a case study. In: *Proceedings of 28th IAHR congress*. Graz, Austria
- Carvalho NO, Filizola JNP, Santos PMC, Lima JEFW (2000) Reservoir sedimentation guideline. Brazilian Electricity Regulatory Agency-ANEEL, Hydrological Studies and Information Department-S.I.H. Brasília Brazil. http://www.aneel.gov.br/biblioteca/downloads/livros/Guia_ava_engl.pdf
- Chia-Yu W, Joann M, Liang M, Mohammad A (2019) Comparison of different spatial interpolation methods for historical hydrographic data of the lowermost Mississippi River. *Ann GIS* 25(2):133–151. <https://doi.org/10.1080/19475683.2019.1588781>
- Childs C (2004) Interpolating surfaces in ArcGIS. *Arcuser* 32–35
- Chung SW, Hipsey MR, Imberger J (2009) Modelling the propagation of turbid density inflows into a stratified lake: Daecheong Reservoir Korea. *Environ Model Software* 24(12):1467–1482. <https://doi.org/10.1016/j.envsoft.2009.05.016>
- Conner JT, Tonina D (2014) Effect of cross-section interpolated bathymetry on 2D hydrodynamic model results in a large river. *Earth Surf Proc Land* 39(4):463–475. <https://doi.org/10.1002/esp.3458>
- David BG (2017) Dams-classification of dams, dam construction, impact of dams: science encyclopedia. Science and Philosophy
- de Jong CD, Lachapelle G, Skone S, Elema IA (2003) *Hydrography 2nd edn*. eBook with corrections January 2010. Delft University Press, The Netherlands. 315–335

- Eakins BW, Grothe PR (2014) Challenges in building coastal digital elevation models. *J Coastal Res* 30(5):942–953
- EL-Hattab AI (2014) Single beam bathymetric data modelling techniques for accurate maintenance dredging. *Egyptian J Remote Sens Space Sci* 17(2):189–195. <https://doi.org/10.1016/j.ejrs.2014.05.003>
- Environmental Protection Agency – E.P.A. (1976) Erosion and sediment control Washington: surface mining in the Eastern U.S. v.1. EPA/625/3–76/006a. Retrieved on 27th September, 2020
- ESRI 2010c ArcGIS Desktop Help 10.0 – TIN to Raster (3D Analyst). <http://help.arcgis.com/en/arcgisdesktop/10.0/help/index.html//00q900000077000000>
- Estigoni M, Matos A, Mauad F (2014) Assessment of the accuracy of different standard methods for determining reservoir capacity and sedimentation. *J of Soils Sediments* 14:1224–1234. <https://doi.org/10.1007/s11368-013-0816-x>
- Farrira IO, Dalto DR, Gérson RS, Lidiane MF (2017) In bathymetric surfaces I D W Or Kriging B C G. *Bull Geodetic Sci* 23(3):493–508. <https://doi.org/10.1590/S1982-21702017000300033>
- Ferrari R, Collins K. (2006) Reservoir survey and data analysis. In: Yang CT (Org.) Erosion and sedimentation manual, U. S. Department of the Interior, Bureau of Reclamation, Denver – Colorado, USA.
- Floriani LD, Magillo P (2009) Triangulated irregular network. In: L.I.U. L., ÖZSU M.T. (eds) Encyclopedia of database systems. Springer, Boston, MA. https://doi.org/10.1007/978-0-387-39940-9_4378
- Girish G, Ashitha MK, Jayakumar KV (2014) Sedimentation assessment in a multipurpose reservoir in Central Kerala. *India Environ Earth Sci* 17(11):4441–4449. <https://doi.org/10.1007/s12665-014-3344-0>
- Georgina E, Andy H, Landing B, Dónall C, Peter B, Paul B (2018) Enhancing digital elevation models for hydraulic modelling using flood frequency detection. *Remote Sens Environ* 217:506–522. <https://doi.org/10.1016/j.rse.2018.08.029>
- Guo Q, Li W, Yu H, Alvarez O (2010) Effects of topographic variability and Lidar sampling density on several DEM interpolation methods. *Photogramm Eng Remote Sens* 76(6):701–712. <https://doi.org/10.14358/PERS.76.6.701>
- Hare R, Eakins B, Amante C (2011) Modelling bathymetric uncertainty. *International Hydrographic Review* 6: 31–42. <https://journals.lib.unb.ca/index.php/ihr/article/view/20888>
- Hengl T (2007) A practical guide to geostatistical mapping of environmental variables. Printed in Italy. EUR 22904 EN – 2007
- Hu K, Li B, Lu Y, Zhang F (2004) Comparison of various spatial interpolation methods for nonstationary regional soil mercury content. *Environ Sci* 25(3):132–137
- Ingham AE (1984) Hydrography for the surveyor and engineer. John Wiley & Sons, New York
- IHO (2011) Manual on hydrography. International Hydrographic Organization Publication C-13. Int Hydrogr Bureal Monaco.
- Ibrahim PO, Sternberg H (2021) Bathymetric survey for enhancing the volumetric capacity of Tagwai Dam in Nigeria via leapfrogging approach. *Geomatics* 1:246–257. <https://doi.org/10.3390/geomatics1020014>
- Isaaks EH, Srivastava RM (1989) Applied Geostatistics. Oxford University Press, New York, USA
- Jahanshir M, Manouchehr H, Sayed-Farhad M, Amir HH (2009) Derivation of reservoir's area-capacity equations. *Am Soc Civil Eng* 14(9):1017–1023. [https://doi.org/10.1061/\(ASCE\)HE.1943-5584.0000074](https://doi.org/10.1061/(ASCE)HE.1943-5584.0000074)
- Kaveh K, Hossein Janzadeh H, Hosseini K (2013) A new equation for calculation of reservoir's area-capacity curves. *KSCE J Civil Eng* 17(10):149–1156. <https://doi.org/10.1007/s12205-013-0230-3>
- Keigo N, Klement T, Amano K (2006) River and wetland restoration: lessons from Japan. *BioScience* 56(5):419–429. [https://doi.org/10.1641/0006-3568\(2006\)056\[0419:RAWRLF\]2.0.CO;2](https://doi.org/10.1641/0006-3568(2006)056[0419:RAWRLF]2.0.CO;2)
- Nakamura K, Tockner K, Amano K (2006) River and wetland restoration: lessons from Japan. *Bioscience* 56(5):419–429. [https://doi.org/10.1641/0006-3568\(2006\)056\[0419:RAWRLF\]2.0.CO;2](https://doi.org/10.1641/0006-3568(2006)056[0419:RAWRLF]2.0.CO;2)
- Khattab MFO, Abo RK, Al-Muqdad SW, Merkel BJ (2017) Generate reservoir depths mapping by using digital elevation model: a case study of Mosul Dam Lake, Northern Iraq. *Adv Remote Sens* 6:161–174. <https://doi.org/10.4236/ars.2017.63012>
- Lampe DC, Morlock SE (2007) Collection of bathymetric data along two reaches of the Lost River within Blue spring Cavern near Bedford, Lawrence County, Indiana. U.S. G. S. Scientific Investigations Report 2008–5023, 142. <http://pubs.water.usgs.gov/sirgt;2008-5023>
- Landim PMB, Sturaro JR, Monteiro RC (2000) Krigagem ordinária para situações com tendência regionalizada. *Revista Laboratório Geomat* 06–12.
- Lark RM (2009) Kriging a soil variable with a simple nonstationary variance model. *J Agric Biol Environ Stat* 14(3):301–321
- Lee J (1991) Comparison of existing methods for building triangular irregular network, models of terrain from grid digital elevation models. *Int J Geogr Inf Syst* 5(3):267–285. <https://doi.org/10.1080/02693799108927855>
- Li J, Heap AD (2008) A review of spatial interpolation methods for environmental scientists. *Geoscience Australia Record* 2008/23.
- Ludek B, Petra S, Petr M, Radek R, Stepan M (2019) River bathymetry model based on floodplain topography. *J Water* 11:1287–1304. <https://doi.org/10.3390/w11061287>
- Marcelo C, Joaquim L, Igor O, Joao L, Jose S (2015) Assessment of spatial interpolation methods to map bathymetry of an Amazonian hydroelectric reservoir to aid in decision marking for water management. *ISPRS Int J Geo-Informatics* 4:220–235. <https://doi.org/10.3390/ijgi4010220>
- Marian M, Dongsu K, Venkatesh M (2012) Gravel bed: processes, tools, environmental; modern digital instruments and morphologic characterization of river channels. John Wiley & Sons, UK
- National Oceanic and Atmospheric Administration. Center for Operational Oceanographic Products and Services. Tide data – station selection. Accessed October 2007 at http://tidesandcurrents.noaa.gov/station_retrieve.shtml?type=Tide+Data
- NOAA (2016) Estimation of vertical uncertainties in VDatum. http://vdatum.noaa.gov/docs/est_uncertainties.htmlhttps://coast.noaa.gov/data/digitalcoast/pdf/topo-bathy-data-considerations.pdf
- Olender HA (1980) Analysis of a triangulated irregular network (TIN) terrain model for military applications. S.R.I. International, final report (1–98). Retrieved online on 08/11/2020.
- S-32 IHO: Hydrographic dictionary-glossary of ECDIS related terms. iho-ohi.net/S32/engview.php
- Samaila-ija HA, Ajayi OG, Zitta N, Odumusu JO, Adesina EA, Ibrahim PO (2014) Bathymetric survey and volumetric analysis for sustainable management: case study of Suleja Dam Niger State Nigeria. *J Environ Earth Sci* 4(18):ISSN 2224-ISSN 3216
- SBADMT,2002. <https://www.discountpdh.com/wp-content/themes/discountpdh/pdf-course/single-beam-acoustic-depth-measurement-techniques.pdf>. Retrieved on 12th July, 2020.
- Silveira TA, Portugal JL, Sá LACM, Vital SRO (2014) Análise estatística espacial aplicada a construção de superfícies batimétricas. *Geociências* 33(4):596–615
- Temitope BO, Kehinde AG (2019) Bathymetric survey and topography changes investigation of part of Badagry Creek and Yewa River, Lagos State, Southwest Nigeria. *J Geogr Environ Earth Sci Int* 22(4):1–16. <https://doi.org/10.9734/jgeesi/2019/v22i430153>

- Thomas EJ, David DH, Karen LB, Richard JH, Angela TB, Donald FC, Daniel AK, David JV (2002) Dam removal: challenges and opportunities for ecological research and river restoration: we develop a risk assessment framework for understanding how potential responses to dam removal vary with dam and watershed characteristics, which can lead to more effective use of this restoration method. *Bioscience* 52(8):669–682. [https://doi.org/10.1641/0006-3568\(2002\)052\[0669:DRCAOF\]2.0.CO;2](https://doi.org/10.1641/0006-3568(2002)052[0669:DRCAOF]2.0.CO;2)
- Urick RJ (1983) Principles of underwater sound, 3rd edn. McGraw-Hill, New York, USA
- Vicente-Serrano SM, Saz-Sánchez MA, Cuadrat JM (2003) Comparative analysis of methods in the middle Ebro Valley (Spain): application to annual precipitation and interpolation temperature. *Climate Res* 24:161–180
- Wechsler SP (2007) Uncertainties associated with digital elevation models for hydrologic applications: a review. *Hydrol Earth Syst Sci* 11:1481–1500
- Wong GSK, Zhu S (1995) Speed of sound in seawater as a function of salinity, temperature, and pressure. *J Acoustical Soc America* 97(3):2020. <https://doi.org/10.1121/1.413048>. Retrieved on 27th October
- Xavier L (2010) An introduction to underwater acoustics: principles and applications, 2nd edn. Springer, Praxis Publishing, Chichester, UK